Journal of Magnetism and Magnetic Materials 382 (2015) 1–6

Contents lists available at ScienceDirect

Journal of Magnetism and Magnetic Materials

journal homepage: www.elsevier.com/locate/jmmm

Structural evolution and enhanced magnetization of $Bi_{1-x}Pr_xFeO_3$

Jing Zhang [a,b], Yu-Jie Wu [c,b], Xiao-Jia Chen [d,*]

[a] School of Mathematics and Physics, Beijing Institute of Technology, Zhuhai 519088, China
[b] Department of Physics, South China University of Technology, Guangzhou 510640, China
[c] School of Physics and Electronic Engineering, Guangzhou University, Guangzhou 510006, China
[d] Center for High Pressure Science and Technology Advanced Research, Shanghai 201203, China

ARTICLE INFO

Article history:
Received 30 October 2014
Received in revised form
11 January 2015
Accepted 23 January 2015
Available online 26 January 2015

Keywords:
Multiferroic materials
Structural transition
Magnetic property

ABSTRACT

The structural, ferroelectric, vibrational, and magnetic properties of polycrystalline $Bi_{1-x}Pr_xFeO_3$ ($0 \le x \le 0.50$) powders are investigated by the measurements of X-ray diffraction, X-ray photoelectron spectroscopy, Raman scattering spectroscopy, and magnetization at room temperature. Our results reveal that the rare-earth ion Pr substitution at Bi site causes the structural transformations from rhombohedral *R*3*c* phase to orthorhombic *Pbam* phase at $x \approx 0.15$, and then to orthorhombic *Pnma* phase at higher Pr concentration $x \approx 0.25$, accompanying the ferroelectric–antiferroelectric–paraelectric phase transition. Measurements of magnetic properties confirm that Pr substitution can improve the magnetization of $BiFeO_3$ before approaching the first phase transition. We find that an inverse behavior occurs after passing a maximum across the antiferroelectric–paraelectric phase boundary. We also obtain the unique switching behavior in low magnetic field of $Bi_{0.5}Pr_{0.5}FeO_3$ from the field dependence on magnetization, indicating the existence of the antiferromagnetic ordering.

1. Introduction

In recent years, much attention has been paid to the multiferroic materials which display ferroelectricity, ferromagnetism and/or ferroelasticity simultaneously in a single phase [1], owing to their interesting physical phenomena and considerable potential applications in data storage, sensors and actuators, etc. [2–4]. Among these multiferroics materials, bismuth ferrite ($BiFeO_3$) has been extensively explored because of its ferroelectric transition temperature and antiferromagnetic Néel temperature well above the room temperature [5]. $BiFeO_3$ is a rhombohedrally distorted perovskite with space group *R*3*c* (Ref. [6]) and described as an $a^-a^-a^-$ tilt system in which the FeO_6 octahedra rotate around the $\langle 111\rangle_p$ (where p=pseudocubic) direction [7]. However, the local short-range order of $BiFeO_3$ is *G*-type antiferromagnet with a cycloid spatial spin modulation with a period of 62 nm [8]. In this way, each Fe^{3+} spin is surrounded by six antiparallel spins on the nearest Fe neighbors, preventing the observations of noticeable magnetization [9]. On the other hand, the ferroelectricity of $BiFeO_3$ mainly arises from the Bi site atoms [10] which are not located exactly in the middle between the FeO_6 octahedra as a result of the off-center displacement of Bi^{3+} caused by the presence of 6*s* lone pair electrons [11]. In the Bi-based perovskites, the $6s^2$ electrons of Bi^{3+} hybridize with 2*s* and 2*p* of oxygen to form a space-filling localized lobe, which in turn pushes away its neighboring atoms causing a structural distortion [12]. Both effects help to induce ferroelectricity [11,13]. However, it is always difficult to obtain the spontaneous polarization in bulk $BiFeO_3$ or the good saturated hysteresis loop *P*–*E* due to the large leakage current [14].

Many attempts have been made to improve the ferroelectricity and magnetization in $BiFeO_3$. The effective way to improve the magnetic properties is to offer internal [14–30] and/or external [31–34] stresses to $BiFeO_3$. The internal stress provided by the substitution of rare-earth cations at the Bi-site of $BiFeO_3$ can effectively modulate the crystal structure parameters and destroy the cycloid spin structure. The effect of cation substitution can lead to the release the locked magnetic moment and the improvement of magnetization [14–22]. However, some researchers considered that the enhanced magnetization can be partly attributed to the existence of Fe^{2+} ion and/or the impurity phase $Bi_{25}FeO_{39}$ [23,24]. Therefore, there is still a debate of the mechanism of the magnetization improvement. For ferroelectric property, the recent investigations on $Bi_{1-x}Re_xFeO_3$ (Re=La [25], Nd [26,27], Sm [28,29], Gd [30]) systems showed that an alike $PbZrO_3$ orthorhombic *Pbam* structure with antiferroelectricity appeared stably between the rhombohedral *R*3*c* and the orthorhombic *Pnma* phase boundaries. It is found that the obtained range of *Pbam* phase in $Bi_{1-x}Re_xFeO_3$ compounds is very narrow due to the smaller ionic radius of Re^{3+} ion substitutes [26,27,30]. Consequently, it can be assumed that the substitution of Pr^{3+} with larger ionic radius (1.32 Å) at Bi-site

---

[*] Corresponding author.
E-mail address: xjchen@hpstar.ac.cn (X.-J. Chen).

http://dx.doi.org/10.1016/j.jmmm.2015.01.061
0304-8853/© 2015 Elsevier B.V. All rights reserved.

will display a wider and more stable configuration of *Pbam* phase. However, there were very few papers focusing on the Pr-doped $BiFeO_3$ system [35–37], and none of them discovered the $PbZrO_3$-like orthorhombic *Pbam* phase. Kumar et al. [35] found that the structure transition from rhombohedral *R*3*c* to triclinic *P*1 in $Bi_{1-x}Pr_xFeO_3$ ($0 \le x \le 0.15$). Moreover, all reports [35–37] showed that both the polarization and dielectric constant increase with increasing Pr substituted concentration *x*. It was attributed to the reduction of oxygen vacancies resulting from the substitution of high valence Pr^{4+} for Bi^{3+}, and the lattice distortion derived from the difference in ionic radius and electronic structures between Pr and Bi ions [35–37]. However, the simplex influence of structural distortion on the ferroelectric property is still under debate.

In this paper, we aim to exhibit clear images of Pr substituted $BiFeO_3$ compounds within the concentration range of $0 \le x \le 0.5$ through the investigations of the structural, ferroelectric, vibrational, and magnetic properties. The high quality samples enable us to understand better about the relations among the structure, ferroelectricity, and ferromagnetization. We show the evidence for the existence of an antiferroelectric orthorhombic *Pbam* phase between ferroelectric orhombohedral *R*3*c* and paraelectric orthorhombic *Pnma* phases. There is giant magnetization improvement approaching the polar–antipolar–nonpolar phase transitions.

2. Experimental

$Bi_{1-x}Pr_xFeO_3$ powders were synthesized by a tartaric acid ($C_4H_6O_6$) modified sol–gel technique. Appropriate amounts of Bi $(NO_3)_3 \cdot 5H_2O$, $Pr(NO_3)_3 \cdot 6H_2O$, and $Fe(NO_3)_3 \cdot 9H_2O$, were dissolved in dilute nitric acid, and calculated amounts of tartaric acid were added as a complex agent. The resultant solution was evaporated and dried at 150 °C with continuous stirring to obtain xerogel powders. Then the xerogel powders were ground in an agate mortar and subsequently preheated to 300 °C for 1 h to remove excess hydrocarbons and NO_x impurities. Finally, all samples were further annealed at 600 °C for 2 h. Phase analysis and investigation of the crystal structure were performed by x-ray diffraction (XRD) technique using a Bruker D8 ADVANCE diffractometer with Cu *Kα* radiation. X-ray photoelectron spectroscopy (XPS) (ESCA Kratos AUD) was used to determine the oxidation states of Fe and Pr ions in the $Bi_{1-x}Pr_xFeO_3$ powders. Raman spectra were recorded in backscattering geometry with a LABRAM Jobin–Yvon spectrometer using a He–Ne laser of wavelength 633 nm. Magnetic properties were measured by using the Physical Properties Measurement System (PPMS, Quantum Design) at room temperature.

3. Results and discussion

All XRD patterns were refined well using the Fullprof Rietvled method. Fig. 1 shows the results of selected XRD measurements of $Bi_{1-x}Pr_xFeO_3$ ($x=0.04$, 0.20, 0.50) powders. There is no trace of routine impurity phases such as $Bi_2Fe_4O_9$, $Bi_{25}FeO_{40}$ and/or Pr_6O_{11} in all samples, indicating a balanced proportion between Bi/Pr and Fe. $BiFeO_3$ is well defined as rhombohedral *R*3*c* symmetry at room temperature, and the unit cell parameters are $a=b=5.57036$ Å and $c=13.84314$ Å.

For Pr-substituted concentration $x \le 0.125$, the XRD patterns can be well refined using a polar rhombohedral *R*3*c* model as shown in Fig. 1(a). There are some new diffraction peaks appearing around $2\theta \approx 17.7°$, 28.9° and 33.0°at $x=0.15$, which indicate a structure transition. A thorough analysis of the diffraction spectra indicated the second phase can be well described using the $PbZrO_3$-like orthorhombic *Pbam* symmetry structure which is characteristic of $\sqrt{2}a \times 2\sqrt{2}a \times 2a$ (where *a* is the pseudocubic lattice parameter, $a \sim 4$ Å) supercell [38]. The space group *Pbam* combines antiphase rotations of the BO_6 octahedra described by $a^-a^-c^0$ tilting system with antipolar displacements of Pb ions along the $\langle 110 \rangle_p$ (where *p* is pseudocubic) axis [26,38]. The fit at $0.15 \le x \le 0.25$ with *Pbam* was very satisfactory, in which we replaced the Pb ions with Bi and Pr ions in the $PbZrO_3$ space group model. This confirms the phase transformation observed around $x=0.15$ is from rhombohedral *R*3*c* symmetry to orthorhombic *Pbam* phase accompanying a ferroelectric–antiferroelectric phase transition. With increasing the Pr concentration *x*, the characteristic peaks (110), (130) and (112) of the orthorhombic *Pbam* phase disappeared above $x=0.25$, while the characteristic diffraction peak around 25° of *Pnma* appeared. It suggests another structure transformation from *Pbam* to *Pnma*. The selected $Bi_{0.50}Pr_{0.50}FeO_3$ sample is well refined using a *Pnma* cell with $a=5.57675$ Å, $b=7.814$ Å, and $c=5.49668$ Å. The space group *Pnma* is a centrosymmetry structure with a paraelectric ordering, and has an $a^-a^-c^+$ tilting system with $\sqrt{2}a \times 2a \times \sqrt{2}a$ supercell [39], which implied that the second structure transition accompanied the antiferroelectric–paraelectric phase transformation.

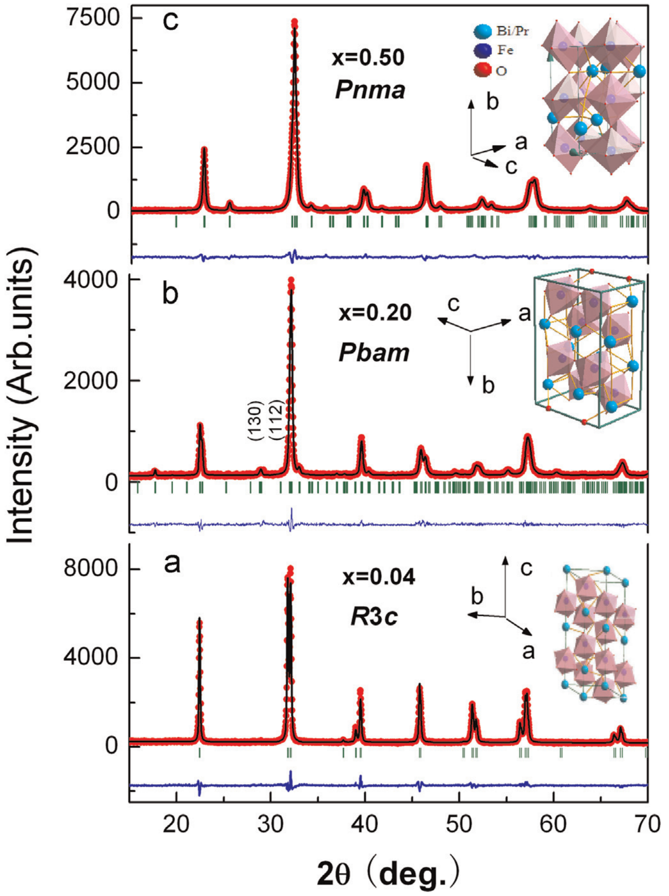

Fig. 1. Observed, calculated, and difference XRD patterns for (a) $Bi_{0.96}Pr_{0.04}FeO_3$, (b) $Bi_{0.80}Pr_{0.20}FeO_3$, and (c) $Bi_{0.50}Pr_{0.50}FeO_3$ samples at room temperature. The refined space groups are given. The insets show schematic representations of the corresponding structures (*R*3*c*, *Pbam*, and *Pnma*, respectively).

Notably, the existence range of *Pbam* phase in $Bi_{1-x}Pr_xFeO_3$ ($0.15 \le x \le 0.25$) powders is broader than that in $Bi_{1-x}Nd_xFeO_3$ and $Bi_{1-x}Sm_xFeO_3$ [26,27,30]. There was even no single *Pbam* phase existed particularly in $Bi_{1-x}Gd_xFeO_3$ and $Bi_{1-x}Dy_xFeO_3$ samples [23,30]. This is attributed to the radius of Pr^{3+} ion (1.32 Å) is larger than Nd^{3+} (1.31 Å), Sm^{3+} (1.28 Å), Gd^{3+} (1.27 Å), and Dy^{3+} (1.24 Å) ions. Also it is the nearest one to the radius of Bi^{3+} ion.